

1  
2  
3  
4  
5  
6  
7  
8  
9  
10  
11  
12  
13  
14  
15  
16  
17  
18  
19  
20  
21  
22  
23  
24  
25  
26  
27  
28

**Title:** *N*-chlorotaurine, a novel inhaled virucidal antiseptic is highly active against respiratory viruses including SARS-CoV-2 (COVID-19)

**Authors:**

Michaela Lackner<sup>1</sup>, Annika Rössler<sup>2</sup>, André Volland<sup>2</sup>, Marlena Stadtmüller<sup>3</sup>, Brigitte Müllauer<sup>2</sup>, Zoltan Banki<sup>2</sup>, Johannes Ströhle<sup>1</sup>, Angela Luttick<sup>4</sup>, Jennifer Fenner<sup>4</sup>, Heribert Stoiber<sup>2</sup>, Dorothee von Laer<sup>2</sup>, Thorsten Wolff<sup>3</sup>, Carsten Schwarz<sup>5</sup>, Markus Nagl<sup>1\*</sup>

<sup>1</sup>Institute of Hygiene and Medical Microbiology, Medical University of Innsbruck, Innsbruck, Austria

<sup>2</sup>Institute of Virology, Medical University of Innsbruck, Innsbruck, Austria

<sup>3</sup>Unit 17-Influenza and Other Respiratory Viruses, Robert Koch-Institute, Berlin, Germany.

<sup>4</sup>360biolabs Pty Ltd, Melbourne, Australia

<sup>5</sup>Christiane Herzog Zentrum Berlin/Charité-Universitätsmedizin Berlin, Berlin, Germany

Co-senior-authors DvL, TW, CS, MN

\*Corresponding author:

Markus Nagl, Assoc.Prof., MD  
Institute of Hygiene and Medical Microbiology  
Medical University of Innsbruck  
Schöpfstr. 41  
A-6020 Innsbruck / Austria

29 Tel. +43-(0)512-9003-70708

30 Fax +43-(0)512-9003-73700

31 E-mail: m.nagl@i-med.ac.at

32 ORCID: 0000-0002-1225-9349

## 33 Abstract

34 *N*-chlorotaurine (NCT) is a long-lived oxidant generated in activated cells of the innate  
35 immune system, namely neutrophilic and eosinophilic granulocytes and monocytes. NCT  
36 acts as an antiseptic agent that can be synthesized chemically and applied topically on  
37 different infected body sites. Even treatment of the lower respiratory tract via inhalation,  
38 which has been in development in the last years, was well tolerated in a recent phase I  
39 clinical trial. In this study, we demonstrate the activity of NCT against viruses causing acute  
40 respiratory tract infections, in fact severe acute respiratory syndrome coronavirus 2 (SARS-  
41 CoV-2), influenza viruses, and respiratory syncytial virus.

42 NCT revealed broad virucidal activity against all viruses tested. In the presence of organic  
43 proteinaceous material simulating body fluids, this activity was enhanced by transchlorination  
44 mechanisms so that significant inactivation of viruses could be achieved within 1 – 10  
45 minutes.

46 Inhalation of 1.0% NCT as a prophylactic and therapeutic strategy against acute viral  
47 respiratory tract infections deserves comprehensive clinical investigation.

48

**49 Introductory paragraph***50 Background*

51 The coronavirus disease 2019 (COVID-19) pandemic is the major challenge of humanity  
52 presently. No highly effective treatment or a vaccine is available so far. Application of *N*-  
53 chlorotaurine (Cl-NH-CH<sub>2</sub>-CH<sub>2</sub>-SO<sub>3</sub>Na, NCT), a safe, well tolerated, endogenous, mild  
54 antiseptic with anti-inflammatory properties may be a significant step forward to combat  
55 COVID-19 and other viral respiratory tract infections. NCT as an inhaled anti-infective has  
56 already demonstrated broad-spectrum microbicidal activity against bacteria, fungi, viruses  
57 and protozoa. Here, we aimed to establish the virucidal activity of NCT against three main  
58 viruses responsible for lower respiratory tract infections, namely severe acute respiratory  
59 syndrome coronavirus 2 (SARS-CoV-2), influenza A virus, and respiratory syncytial viruses  
60 (RSV).

61

62 The COVID-19 pandemic is caused by SARS-CoV-2. The pandemic is affecting individuals,  
63 populations, and health systems far beyond infection. The virus might persist globally and  
64 become a prolonged or permanent threat <sup>1,2</sup>. Up to date, there is no breakthrough regarding  
65 a highly sufficient and well tolerated prophylaxis, vaccine or therapy. The race for a cure is a  
66 global effort and different approaches have been developed and are currently studied <sup>1,3</sup>.

67 Another major public concern is posed by influenza viruses, which annually cause 3 – 5  
68 million cases of severe illness and about 290 000 to 650 000 of death worldwide <sup>4</sup>. Protection  
69 by the yearly influenza virus vaccine is unsatisfactory and resistance against existing antiviral  
70 drugs develops rapidly <sup>5</sup>. Therefore, new tools to combat influenza viruses are urgently  
71 needed.

72 One less known intervention is inhalation therapy with antiviral agents. An appeal for the  
73 inhaled route of administration has been published recently <sup>6</sup>. A first advantage is direct  
74 delivery of a high concentration of the medication to the lung, where the virus causes most of  
75 the severe problems <sup>7</sup>. Furthermore, topically applied therapies that are not systemically  
76 distributed avoid interactions with systemic medications, which are frequently necessary in

77 elderly or multimorbid patients who are particularly at risk for severe COVID-19 complications  
78 <sup>8</sup>. An ideal inhaled drug should have broad-spectrum antimicrobial activity to cover not only  
79 SARS-CoV-2, but also co-infections and superinfections with other respiratory viruses and  
80 microorganisms (bacteria and fungi) <sup>9-11</sup>. Antiviral drugs are often specific to distinct viruses,  
81 but identifying the virus causing an infection requires logistic and diagnostic efforts, which in  
82 the case of SARS-CoV-2 amounts to at best one to two days for a diagnosis<sup>12</sup>. Such an ideal  
83 inhaled broad-spectrum drug mentioned above could be applied instantly regardless of the  
84 pathogen causing the respiratory illness and would thus eliminate the need for time-  
85 consuming diagnostics. Another key requirement is anti-inflammatory activity of the  
86 compound to downregulate the 'cytokine storm', particularly for SARS-CoV-2, which causes  
87 hyper-inflammation in severe cases <sup>13</sup>.

88 One molecule that fulfils the criteria of broad-spectrum antimicrobial (virucidal,  
89 bactericidal, fungicidal, protozoocidal) and anti-inflammatory activity <sup>14,15</sup>, and good  
90 tolerability upon inhalation is *N*-chlorotaurine (Cl-NH-CH<sub>2</sub>-CH<sub>2</sub>-SO<sub>3</sub><sup>-</sup>) <sup>16</sup>. It is known since the  
91 1970's as a product of activated human granulocytes and monocytes and belongs to the  
92 long-lived oxidants and chloramines formed by the myeloperoxidase via hypochlorous acid to  
93 combat invading pathogens <sup>17-19</sup> (Fig. 1). Moreover, *N*-chlorotaurine is thought to be involved  
94 in the control of inflammation by downregulating of nuclear factor kappaB activation,  
95 chemokines and proinflammatory cytokines such as tumor necrosis factor alpha, some  
96 prostaglandins and interleukins like IL-6 <sup>15,20,21</sup>. The synthesis of the sodium salt of *N*-  
97 chlorotaurine (Cl-NH-CH<sub>2</sub>-CH<sub>2</sub>-SO<sub>3</sub>Na, NCT) was successful in our laboratory <sup>22</sup>, which  
98 enabled its development as an endogenous anti-infective and mild antiseptic in human  
99 medicine. As an active chlorine compound belonging to the class of chloramines, it has the  
100 typical broad-spectrum microbicidal activity without development of resistance against Gram-  
101 positive and Gram-negative bacteria including multi-resistant strains, yeasts and moulds,  
102 protozoa, and worm larvae (for review see <sup>14,23,24</sup>). Broad-spectrum activity was found against  
103 adenoviruses <sup>25-27</sup>, herpes viruses 1 and 2 <sup>26,27</sup>, human immunodeficiency virus <sup>28</sup>, and it was  
104 shown *in vivo* against adeno and herpes viruses in epidemic keratoconjunctivitis up to a

105 phase II study as well as in herpes zoster in a case report, respectively <sup>29-31</sup>. Activity against  
106 coxsackievirus A24 and enterovirus 70 was found by the NCT-derivative *N,N*-dichloro-  
107 dimethyltaurine *in vitro* <sup>32</sup>.

108 In the last years, inhalation of NCT has been investigated and developed in detail.  
109 Enhanced bactericidal and fungicidal activity has been found in the presence of lung  
110 epithelial cells <sup>33</sup>. Tolerability of repeatedly inhaled NCT has been confirmed in the normal  
111 lung and in a streptococcal inflammation model each in pigs, and in the normal lung of mice  
112 <sup>34-36</sup>. In humans, tolerability was confirmed in a placebo-controlled phase I clinical study <sup>16</sup>.  
113 Only minor and transient adverse effects were found, i.e. chlorine taste and occasional tickle  
114 in the throat <sup>16</sup>. NCT is not distributed systemically, which explains the absence of systemic  
115 adverse effects.

116 A safe, well tolerated, endogenous, inhaled substance with broad-spectrum activity  
117 against pathogens supported by anti-inflammatory properties may be a significant step  
118 forward for treatment of COVID-19 and other viral infections of the lower airways without the  
119 need of further diagnostics to discriminate between the infectious agents. In this regard, the  
120 aim of the present study was to establish and characterize the virucidal activity of NCT  
121 against three major viruses responsible for respiratory infections in humans, namely SARS-  
122 CoV-2, influenza viruses, and RSV *in vitro*.

123

## 124 **Results**

125

126 NCT was incubated with SARS-CoV-2, influenza A virus or RSV, followed by assessment of  
127 virus inactivation using various readouts. NCT at a clinically relevant concentration of 0.1% -  
128 1.0% demonstrated virucidal activity against SARS-CoV-2 (SARS-CoV-2 BavPat1, hCoV-  
129 19/Australia/VIC01/2020, clinical isolate 1.2 Innsbruck), influenza A virus, and RSV (RSV  
130 long strain). Longer NCT-exposure periods were required to inactivate SARS-CoV-2 than to  
131 inactivate influenza viruses or RSV. In the presence of organic matter, inactivation of viruses  
132 was even enhanced so that a significant reduction of plaque forming units and infected cells,

133 respectively, could be observed already after 5 min with SARS-CoV-2 by 1.0% NCT.  
134 Controls without NCT and specific inactivation controls showed full viral replication in all  
135 cases to warrant valid results. Detailed results are presented in the following paragraphs.

136

### 137 **Virucidal activity of NCT against SARS-CoV-2**

138

139 Inactivation of SARS-CoV-2 was assessed by incubating stock virus with NCT for indicated  
140 time periods at 37°C and then determining the remaining infectious particles using plaque  
141 assay or immunostaining as well as determining virus inactivation via RT-qPCR or TCID50.  
142 Exact incubation times of virus with NCT were ensured by adding met/his at the end of the  
143 incubation period, which inactivates NCT. All assays demonstrated a significant inactivation  
144 of SARS-CoV-2 with slight differences according to the individual test method and strain  
145 used. With plaque assay readout, a significant reduction in infectious particles was detected  
146 after 15 min of incubation, when incubating SARS-CoV-2 with NCT in a buffered aqueous  
147 solution (Fig. 2a). The mild oxidizing activity of the test antiseptic may explain why it took as  
148 long as 15 min to reduce infectious particles. In the presence of Vero cells (Fig. 2b) or  
149 particularly 5.0% peptone (Fig. 2a), however, a significant reduction of infectious virus  
150 particles occurred already after 5 min of incubation with 1.0% NCT. This remarkable  
151 enhancement of activity by organic load is typical for NCT and shown for viruses for the first  
152 time here and is explained most likely by transhalogenation (see discussion).

153 Virus inactivation assays with immunostaining readout showed a 50% reduction of infected  
154 cells after 1 min (not significant,  $p = 0.085$ ), 20 – 80% reduction after 5 min ( $p = 0.0102$ ), 81 –  
155 91% after 7 min ( $p < 0.01$ ), 81 – 97% after 10 min, 96 – 99% after 20 min, and > 99% after  
156 30 min ( $p < 0.0001$  for these values). A logarithmic scale with respective statistics is provided  
157 in Fig. 2c. The results found by RT-qPCR assay were similar with a highly significant  
158 reduction of genome copies (Fig. 2d). This was further confirmed by the TCID50 readout  
159 (Fig. 2e).

160 The antiviral activity was concentration-dependent. Inactivation controls demonstrated full  
161 inactivation of 1.0% NCT by 1.0% methionine / 1.0% histidine (met/his). This was valid for all  
162 tests and viruses in this study. Absence of cytotoxicity of inactivated NCT to the inoculated  
163 cell culture was proved by MTT testing with values of MTT reduction of  $94.1 \pm 8.5$  (0.1% NCT  
164 plus 0.1% met/his) and  $100.3 \pm 5.6$  (PBS control) ( $p = 0.12$  by Student's unpaired t-test).

165

### 166 **Virucidal activity of NCT against influenza viruses**

167

168 Inactivation of influenza viruses was assessed like inactivation of SARS-CoV-2 by incubating  
169 stock virus with NCT for indicated time periods at 37°C and then determining the remaining  
170 infectious particles using plaque assay.

171 Virus inactivation as determined by plaque assay readout demonstrated an even faster  
172 inactivation of influenza viruses by NCT compared to SARS-CoV-2. All tested virus strains  
173 were inactivated rapidly with a 2  $\log_{10}$  reduction of the H3N2 virus within 5 min (Fig. 3a) and a  
174 6  $\log_{10}$  reduction of H1N1 and H1N1pdm viruses within 1 min by 1.0% NCT (Fig. 3b and 3c).

175 In general, H1N1 and H1N1pdm viruses were more susceptible than the H3N2 virus.

176 Addition of ammonium chloride ( $\text{NH}_4\text{Cl}$ ) to NCT significantly enhanced its activity against  
177 influenza viruses (Fig. 3d). Ammonium chloride alone and the inactivation control with 0.1%  
178 NCT plus 0.1% ammonium chloride showed no antiviral effect at least up to 10 min  
179 incubation time.

180

### 181 **Virucidal activity of NCT against RSV**

182 Inactivation of RSV was assessed like inactivation of SARS-CoV-2 and influenza A viruses.

183 As with SARS-CoV-2 and influenza A virus, inactivation of RSV as determined by plaque  
184 assay readout demonstrated a significant reduction of PFU/ml by NCT compared to mock  
185 treated controls. The incubation of RSV with 1.0% NCT resulted in a rapid drop of infectious  
186 virus titre with 4  $\log_{10}$  decrease within 5 minutes (Fig. 4). Almost no detectable amount of  
187 infectious RSV was measurable after 15 minutes. In the presence of 0.1% NCT, RSV titres



188 dropped in a time- and concentration-dependent manner reaching significant titre reduction  
189 after 15 minutes (Fig. 4).

190

## 191 **Discussion**

192 Safe, well tolerated, affordable, and effective medications are urgently needed against  
193 COVID-19 and would be beneficial for treatment of viral bronchopneumonia caused by other  
194 viruses such as influenza and RSV. As an endogenous mild long-lived oxidant <sup>17</sup>, inhaled  
195 NCT has been demonstrated to be well tolerated and safe in animals (pigs and mice) and in  
196 a clinical phase I study in humans <sup>16,34-36</sup>. As an active chlorine compound belonging to the  
197 class of chloramines, it has broad-spectrum activity against pathogens without occurrence of  
198 resistance because of the oxidizing mechanism of activity with thio- and amino-groups as the  
199 main targets <sup>14,22,23</sup>.

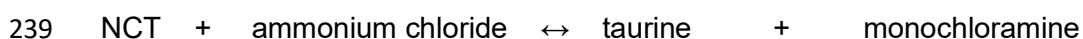
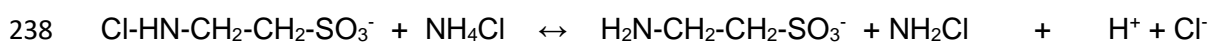
200         Actually, in the present study NCT had clear virucidal activity against three enveloped  
201 RNA viruses highly relevant for infections of the bronchopulmonary system. Depending on  
202 the NCT-concentration and test conditions, a rapid reduction of the number of infectious virus  
203 particles by several powers of ten within 1 - 10 minutes is achieved. Influenza A viruses of  
204 pre-pandemic and pandemic H1N1 subtype (H1N1 and H1N1pdm) were the most sensitive  
205 ones with reduction to the detection limit by 1.0% NCT within 1 min, followed by RSV,  
206 influenza (H3N2), and SARS-CoV-2. These differences can be explained by individual  
207 dynamics of oxidation and chlorination of proteins of the viral surface, and of penetration of  
208 NCT and attack on the viral nucleocapsid proteins. All these target sites have been shown  
209 with the NCT analogue *N,N*-dichloro-2,2-dimethyltaurine in adenovirus type 5 <sup>37</sup>. Thereby,  
210 chlorination of the surface proteins is the first step <sup>38</sup>, which can be assumed to impact their  
211 function and therefore the attachment of viruses to body cells. Oxidation and chlorination of  
212 virulence factors of different pathogens by NCT and analogue chloramines with the  
213 consequence of their inactivation has been also shown for shigatoxin of *Escherichia coli* <sup>39</sup>,  
214 several toxins of *Staphylococcus aureus* <sup>40</sup>, aspartyl proteinases of *Candida spp.* and  
215 gliotoxin of *Aspergillus fumigatus* <sup>41,42</sup>. This indicates that inactivation of key proteins of all

216 kinds of pathogens is a central principle of the antimicrobial action of NCT and may underline  
 217 such a function in innate immunity besides its anti-inflammatory one <sup>15,20,23</sup>.

218 Accordingly, NCT has not only virucidal activity against enveloped viruses (herpes  
 219 virus type 1 and 2 <sup>26,27</sup>, human immunodeficiency virus 1 <sup>28</sup>, and the viruses of the present  
 220 study), but also non-enveloped ones. From the latter, a panel of adenoviruses has been  
 221 tested mainly due to their importance in epidemic keratoconjunctivitis <sup>25,27,30</sup>. Similar to other  
 222 active halogen compounds and other antiseptics such as tensidic compounds <sup>43</sup>,  
 223 adenoviruses are slightly less sensitive to NCT than the enveloped viruses <sup>27</sup>. Nevertheless,  
 224 efficacy of NCT *in vivo* against adenoviruses in epidemic keratoconjunctivitis has been  
 225 proven in the New Zealand White rabbit ocular model and in a phase II study in humans <sup>30,31</sup>.  
 226 Application of NCT had a curative effect in a patient suffering from therapy-refractory herpes  
 227 zoster infection in the upper thoracic area <sup>29</sup>.

228 It must be taken into account that organic substances are omnipresent *in vivo* (in all  
 229 human body fluids and tissues), and therefore we performed a part of the inactivation assays  
 230 in the presence of organic matter as well. The results of Fig. 2a clearly show an  
 231 enhancement of the virucidal activity of NCT in the presence of 5.0% peptone, which in the  
 232 first view appears surprising since active chlorine compounds underlie a decrease of their  
 233 oxidation capacity by chlorine-reducing substances of such organic load <sup>23,44,45</sup>. With NCT as  
 234 a low-reactive chloramine compound, however, transchlorination as one of the reaction  
 235 mechanisms becomes important <sup>14,23</sup>. Thereby, amongst others, monochloramine (NH<sub>2</sub>Cl) is  
 236 formed in equilibrium from NCT and ammonium chloride <sup>14,17</sup>.

237



240

241 Monochloramine is more lipophilic than NCT and penetrates microorganisms more easily,  
 242 which leads to enhanced inactivation by the reaction just mentioned <sup>17,46</sup>. The stronger  
 243 activity of NCT in the presence of fluids containing proteinaceous material is a general

244 principle observed in different compositions, such as artificial sputum medium, different body  
245 fluids, peptone, and plasma for bacteria and fungi (for review see <sup>14,24,47</sup>). In the present  
246 study, it has been confirmed for viruses for the first time, too. The discrepancy between the  
247 incubation time of 15 min (Fig. 2a) and of 10 min or less (Fig. 2b-e) needed for a significant  
248 viral reduction in buffer solution in different tests may be explained by the presence of 1.0%  
249 FCS in the tests depicted in Fig. 2c-e and organic matter in the presence of Vero cells in Fig.  
250 2b. In agreement with these results, enhancement of the bactericidal and fungicidal activity of  
251 NCT in the presence of different lung epithelial cells was observed recently <sup>33</sup>.

252         Enhancement of antimicrobial and antiviral activity by organic material is of practical  
253 relevance for topical treatment of infections with NCT, for instance bronchopulmonary ones.  
254 The concentration of active chlorine after the end of an inhalation of 1.0% NCT decreases to  
255 traces within 1 min and vanishes completely after further 10 min <sup>16</sup>. Inhalation for 10 min is  
256 feasible and well tolerated, and within this time an impact on SARS-CoV-2 and on other  
257 viruses can be expected *in vivo*, too, but remains to be evaluated in respective clinical  
258 studies.

259         Also of practical relevance is the fact that NCT has broad-spectrum activity against  
260 viruses, including important representatives relevant for bronchopulmonary infections  
261 (SARS-CoV-2, influenza viruses, RSV). Topical treatment of all these virus infections by  
262 inhaled NCT without the necessity of a diagnosis of the specific virus at hand is conceivable  
263 and should urgently be investigated in clinical studies. Notably, the activity of NCT against  
264 bacteria and fungi, including multi-resistant ones, may prevent super- and secondary  
265 infections, which are a considerable problem in COVID-19 patients as well <sup>9-11</sup>. In addition,  
266 the anti-inflammatory activity of NCT might have the potential to influence the aggressive  
267 inflammatory response by downregulating the 'cytokine storm' and prevent airway damage in  
268 severe ill patients with SARS-CoV-2 infection.

269 Further advantages of NCT would be high safety and high tolerability by human tissue <sup>14</sup>,  
270 absence of systemic absorption, of systemic adverse effects <sup>16</sup>, of systemic interaction with

271 other medications, and of resistance development because of the oxidizing and chlorinating  
272 mechanism of action <sup>14,23</sup>.

273

## 274 **Conclusions**

275

276 NCT demonstrated rapid activity against SARS-CoV-2, influenza A viruses, and RSV at a  
277 therapeutic concentration of 1.0% that can be safely inhaled. The activity is enhanced by an  
278 organic environment, which is omnipresent in human body fluids and tissues *in vivo*. Clinical  
279 efficacy of NCT in viral bronchopulmonary infections should be investigated in respective  
280 clinical studies.

281

282

## 283 **Methods**

284

### 285 **Reagents**

286

287 *N*-chlorotaurine sodium salt (NCT, molecular weight 181.57 g/l, lot 2020-03-17) was  
288 prepared in pharmaceutical quality as established at our Department and frozen at minus  
289 20°C for storage <sup>22</sup>. For testing, it was freshly dissolved in phosphate-buffered saline (PBS)  
290 at pH 7.1 (7.0 – 7.2) to desired stock concentrations between 1.0% (55.08 mM) and 10%.  
291 As inactivation solution for NCT, a mixture of 1.0% methionine and 1.0% histidine (met/his, L-  
292 methionine and L-histidine, both from Carl Roth GmbH, Karlsruhe, Germany) in distilled  
293 water was used <sup>48</sup>. For tests in peptone, peptone enzymatic digest from Casein was applied  
294 (Fluka no. 82303, Sigma-Aldrich GmbH, Buchs, Switzerland). RPMI-1640 medium and fetal  
295 calf serum (FCS) were from Sigma-Aldrich GmbH, too.

296

## 297 **Viruses, virus cell culture and preparation of viral suspensions**

298

299 **SARS-CoV-2**

300

301 *Robert Koch-Institute, Berlin (RKI)*

302 SARS-CoV-2 BavPat1 strain was obtained from Christian Drosten's laboratory at the Institute  
303 of Virology at Charité Universitätsmedizin Berlin. Vero E6 cells were maintained in DMEM  
304 (supplemented with 10% FCS, 2 mM L-glutamine, non-essential amino acids, 1mM sodium  
305 pyruvate, 100 mg/ml streptomycin and 100 units/ml penicillin). For virus stock preparation,  
306 Vero E6 monolayer cultures grown in 75 cm<sup>2</sup> cell culture flasks were infected with a  
307 multiplicity of infection (MOI) of 0.01 in PBS (supplemented with 0.3% BA) for 2 days at 37°C  
308 and 5.0% CO<sub>2</sub>. The supernatant was harvested and stored at minus 80°C until use.

309

310 *Biolabs, Melbourne (Biolabs)*

311 COVID-19 strain used was SARS-CoV-2 hCoV-19/Australia/VIC01/2020 (Melbourne's Peter  
312 Doherty Institute for Infection and Immunity, Melbourne, Australia). Parent stock of the virus  
313 was passaged twice in Vero cells. A working stock was generated at 360biolabs by two  
314 further passages in Vero cells in virus growth media, which comprised Minimal Essential  
315 Medium without L-glutamine supplemented with 1.0% (w/v) L-glutamine 1.0 µg/ml of TPCK-  
316 Trypsin, 0.2% BSA, 1 x Pen/Strep, and 1.0% Insulin Transferrin Selenium (ITS), then a  
317 further 2 passages in Vero E6 cells in growth media. This growth media comprised MEM  
318 supplemented with 1.0% (w/v) L-glutamine, 4.0 µg/ml of TPCK-Trypsin and 2.0% (v/v) heat  
319 inactivated FBS.

320 African Green Monkey Kidney (Vero E6) cells (ATCC-CRL1586) were sub-cultured to  
321 generate cell bank stocks in cell growth medium, which comprised Minimal Essential Medium  
322 without L-glutamine supplemented with 10% (v/v) heat-inactivated Fetal Bovine Serum and  
323 1.0% (w/v) L-glutamine. Cell stocks were frozen at minus 80°C overnight and then  
324 transferred to liquid nitrogen. Vero E6 cells were passaged for a maximum of 13 passages,  
325 after which a new working cell bank stock was retrieved from liquid nitrogen for further use.  
326 Vero E6 cells were seeded into 96-well plates at 2 x 10<sup>4</sup> cells / well in 100 µl E6 seeding

327 media (Minimal Essential Medium supplemented with 1.0% (w/v) L-glutamine, 2.0% FBS).

328 Plates were incubated overnight at 37°C, 5.0% CO<sub>2</sub>.

329

330 *Institute of Virology, Innsbruck*

331 SARS-CoV-2 Isolate 1.2 was a clinical isolate from a patients' respiratory swab sample in

332 Innsbruck, Austria. Virus stocks were produced on Vero/TMPRSS2 cells, kindly provided by

333 Dr. Markus Hoffmann and Prof. Stefan Pöhlmann, Leibniz Institute for Primate Research,

334 Göttingen, Germany <sup>49</sup>. Cells were cultured in DMEM plus 10% FCS and Pen/Strep. For

335 Virus stock production, 80% confluent Vero/TMPRSS2 cells were infected with a MOI of 0.01

336 in DMEM plus 2.0% FCS. The supernatant was harvested 60 h post infection. Virus aliquots

337 were stored at minus 80°C.

338

### 339 **Influenza**

340

341 *Robert Koch-Institute, Berlin (RKI)*

342 Influenza A/Panama/2007/1999 (H3N2) virus was grown in the allantois cavity of 11 day old

343 embryonated chicken eggs for 2 days. Virus was harvested, clarified by centrifugation

344 (300xg, 10 min) and stored at minus 80°C until use. Madin-Darby-Canine-Kidney (MDCK) II

345 cells (ATCC) were maintained in MEM (supplemented with 10% FCS, 2 mM L-glutamine,

346 100 mg/ml streptomycin and 100 units/ml penicillin) at 37°C and 5.0% CO<sub>2</sub>.

347

348 *Institute of Hygiene and Medical Microbiology, Innsbruck*

349 Influenza A/Singapore/Hongkong/2339/2000 (H1N1) was kindly provided by H. Katinger,

350 Institute of Applied Microbiology, University of Natural Resources and Applied Life Sciences,

351 Vienna, Austria. Influenza A/Swine Origin Virus (S-OIV)/California/2009 (H1N1pdm) was a

352 clinical isolate from Innsbruck, Austria.

353 Influenza viruses were grown on MDCK cells (Collection of Cell Lines in Veterinary Medicine,

354 Friedrich-Loeffler-Institut, Federal Research Institute for Animal Health, Greifswald,

355 Germany). MDCK cells were grown in 25 cm<sup>2</sup> cell culture flasks (Sarstedt, Inc. Newton, NC,  
356 USA) in RPMI plus 10% FCS to a monolayer. The medium was replaced by 5 ml RPMI  
357 without FCS, and 10 µl of 1 mg/ml trypsin (final concentration 0.002 mg/ml) was added to  
358 activate neuraminidase. Viral suspension deep frozen at minus 80°C in RPMI (200 µl) was  
359 added. After 60 h of incubation at 37°C, a cytopathic effect was seen in all cells, and the  
360 supernatant was taken and centrifuged at 275 × g. The supernatant again was used as viral  
361 suspension for the tests.

362

### 363 **RSV**

364 RSV long strain, (kindly provided by T. Grunwald, Fraunhofer Institute for Cell Therapy and  
365 Immunology, Leipzig, Germany), was generated by infection of HEp2 cells at low MOI as  
366 described previously<sup>50</sup>. Virus titers were determined in plaque assays by infection of HEp2  
367 with serial dilutions of the virus followed by immunocytochemical staining with polyclonal goat  
368 antibody against RSV (Gt X RSV, Merck) and HRP-conjugated rabbit polyclonal anti-goat  
369 IgG (Novusbio). 3-Amino-9-ethylcarbazole (AEC, Sigma) was used as a chromogen in  
370 immunohistochemistry to visualize the RSV infected cells.

371

### 372 **Virus inactivation tests (quantitative killing assays) with NCT**

373

#### 374 General overview of the test method

375

376 The viral suspension was mixed with NCT (final concentration 0.1% to 1.0%) and incubated  
377 at 37°C for 1, 5, 7, 10, 15, 20, 30, 45, and 60 min. At the end of each incubation time,  
378 aliquots were removed and diluted in 1.0% met/his to inactivate NCT and to warrant exact  
379 incubation times. Virus inactivation was assessed by subsequent plaque assay,  
380 immunostaining or RT-qPCR as detailed below.

381 Controls were done in PBS or PBS with 5.0% peptone without NCT in parallel as well as

382 inactivation controls. For the latter, 1.0% NCT was mixed with met/his before the addition of

383 the respective virus. The virus must survive in the inactivation solution to obtain reliable  
384 results, which was the case in all tests.

385

386 **SARS-CoV-2**

387

388 Virus inactivation assay with plaque assay readout (RKI Berlin)

389 Three µl of concentrated virus suspension ( $4.76 \times 10^9$  PFU/ml) were added to 400 µl of NCT  
390 (1.0% or 0.1% in PBS), NCT with peptone (1.0% NCT, 5.0% peptone in PBS) or PBS and  
391 incubated at 37°C. After 5, 15, 30 and 60 min, 100 µl were removed and added to 100 µl of  
392 met/his. As inactivation control, 100 µl of 1.0% NCT or 1.0% NCT with 5.0% peptone were  
393 added to 100 µl of met/his and thereafter 0.75 µl of virus suspension were added. Infectious  
394 virus particles in all suspensions were determined with plaque assay. Briefly, a serial tenfold  
395 dilution of the virus suspension in PBS with 0.3% bovine albumin was added to confluent  
396 Vero E6 cells in 12-well plates, which were washed with PBS immediately before. After  
397 incubation at 37°C for 1h, the inoculum was removed followed by a washing step with PBS.  
398 Avicel-overlay medium (double-strength DMEM supplemented with 10% FCS, 1.0% DEAE  
399 dextran, 5.0% sodium bicarbonate and 1.25% Avicel) was added and plates incubated at  
400 37°C and 5.0% CO<sub>2</sub> for 3 days before staining with crystal violet for visualization of plaques.  
401 Counted plaques are expressed as plaque forming units per ml (PFU/ml).

402

403 Virus inactivation assay with plaque assay readout (GLP lab 360 biolabs, Melbourne)

404 Cell seeding media were removed from a pre-seeded plate (assay plate) and cell monolayers  
405 were washed with PBS twice. A volume of 50 µl of non-supplemented MEM was added to all  
406 wells except the isopropanol positive control wells. A volume of 50 µl of (4.0% or 0.4%) NCT  
407 was added to NCT-treated wells, 50 µl of non-supplemented MEM was added to virus only  
408 wells and 100 µl of isopropanol ( $\geq 99.5\%$ , Sigma-Aldrich) added to positive control wells. A  
409 100 µl volume of SARS-CoV-2 (B3) that had been pre-diluted 1:10 in non-supplemented  
410 MEM was added to all wells. Plates were incubated for 5, 10, 20, and 60 min at 37°C, 5.0%



411 CO<sub>2</sub>. An additional 100 µl of virus growth media containing TPCK trypsin required for virus  
412 growth (MEM supplemented with 1.0% (w/v) L-glutamine, 2.0% FBS and 8 µg/ml TPCK  
413 trypsin) was added to plates pre-seeded with Vero E6 cells that samples were to be titrated  
414 onto.

415 At each time point, 100 µl of either 1.0% or 0.1% NCT media was removed from the  
416 assay plate and added to either 100 µl of met/his in distilled water to inactivate the NCT. The  
417 positive control and virus only controls were also diluted 1:2 into distilled water. Each sample  
418 was diluted a further 1:10 into virus growth media, MEM supplemented with 1.0% (w/v) L-  
419 glutamine and 2.0% FBS containing 4.0 µg/ml of TPCK trypsin (i.e. 100 µl of inactivated  
420 sample + 900 µl of virus growth media). The remaining virus after NCT inactivation was  
421 quantified by addition of 100 µl volume of 1:10 diluted inactivated NCT to triplicate wells of  
422 96-well plate pre-seeded with Vero E6 cells. Plates were incubated at 37°C, 5.0% CO<sub>2</sub> for 4  
423 days. Virus-induced CPE was scored visually. The TCID<sub>50</sub> of the virus suspension was  
424 determined using the method of Reed-Muench<sup>51</sup>. The virucidal effect was quantified as the  
425 log<sub>10</sub> reduction in virus titre compared to the SARS-CoV-2 control. Isopropanol (≥ 99.5%) was  
426 used as the assay positive control.

427 For inactivation controls, 100 µl of NCT at 4.0% and 0.4% was added to 100 µl of  
428 4.0% met/his or 0.4% met/his prior to addition of virus. A volume of 100 µl of this inactivation  
429 mix was added to wash pre-seeded Vero E6 cells. To this, 100 µl of virus pre-diluted 1:10 in  
430 non-supplemented MEM was added and incubated at 37°C, 5.0% CO<sub>2</sub> for 10 min or 60  
431 minutes. Following the incubations, 100 µl was diluted into 900 µl of virus growth media  
432 containing 4 µg/ml of TPCK trypsin (1:10). The remaining virus was quantified as outlined  
433 above.

434

435 Absence of cytotoxicity of inactivated NCT to the inoculated cell culture.

436 As a cytotoxicity control, the 1.0% NCT and 0.1% NCT was set up the same and inactivated  
437 by met/his as outlined above but instead of 100 µl of virus being added, 100 µl of non-  
438 supplemented MEM was added. These samples were treated exactly the same as above

439 and titrated across pre-seeded cells to ascertain any cytotoxicity observed by the NCT. For  
440 cell viability staining, a 100 µl volume of a 3 mg/ml solution of 3-(4,5-dimethylthiazole-2-yl)-  
441 2,5-diphenyl tetrazolium bromide (MTT) was added to cytotoxicity control plates and  
442 incubated for 2 h at 37°C in a 5.0% CO<sub>2</sub> incubator. Wells were aspirated to dryness using a  
443 multichannel manifold attached to a vacuum chamber and formazan crystals solubilised by  
444 the addition of 200 µl 100% 2-Propanol at room temperature for 30 minutes. Absorbance was  
445 measured at 540 – 650 nm on a plate reader. Absorbance values were averaged and  
446 reported as % reduction of MTT to formazan.

447

448 Virus inactivation assay with immunostaining and RT-qPCR (Virology Innsbruck).  
449 Each 150 µl of NCT (2.0% in PBS) and of virus suspension (in DMEM plus 2.0% FCS plus 2  
450 mM glutamine, plus Pen/Strep) were mixed and incubated at 37°C. After each incubation  
451 time, 50 µl were removed and transferred to an equal volume of met/his. Controls were done  
452 in PBS without NCT. As inactivation controls, 75 µl of 2.0% NCT in PBS were added to 150  
453 µl of met/his, followed by addition of 75 µl virus suspension. After serial tenfold dilution of this  
454 suspension, 50 µl each were added to 90% confluent Vero/TMPRSS2 or  
455 Vero/TMPRSS2/ACE2 cells in 96-well plates, from which the medium was removed  
456 immediately before. After incubation of 1 h at 37°C, the supernatant was removed, and after  
457 a washing step with 100 µl of medium, 100 µl of fresh medium was added. After further 9 h  
458 incubation, cells were fixed for immunostaining or total RNA was extracted for RT-qPCR as  
459 described below.

460

461 Immunostaining (detection by antibodies and peroxidase-marked second antibody)  
462 After fixation for 5 min with 96% EtOH, cells were blocked for 15 min with PBS containing  
463 0.1% FCS. Subsequently, cells were stained using serum from a SARS-CoV-2 recovered  
464 patient and horse radish peroxidase (HRPO)-conjugated anti-human secondary antibody.  
465 The signal was developed using a 3-amino-9-ethylcarbazole (AEC) substrate. Infected cells  
466 were visible as red spots and the number of infected cells was counted using an

467 ImmunoSpot S6 Ultra-V reader and CTL analyser *BioSpot*® 5.0 software (CTL Europe  
468 GmbH, Bonn, Germany).

469

470 RT-qPCR

471 For RNA extraction, the supernatant was removed, and the cell monolayer was washed twice  
472 with PBS. The cells were lysed 5 min at room-temperature using 100 µl in-house direct lysis  
473 buffer (10 mM Tris-HCL pH 7.4, 25 mM NaCl, 0.5% IGEPAL, 10 Units RiboLock RNase  
474 Inhibitor in DEPC-treated water)<sup>52</sup>. Subsequently, 5 µl RNA was used in a one-step RT-  
475 qPCR assay using the iTaq™ RT-PCR (BIO-RAD) kit and previously published primers and  
476 probes specific for detection of the SARS-CoV-2 E Gene on a CFX96™ real-time system  
477 (BIO-RAD)<sup>53</sup>.

478

479 Virus titration by TCID<sub>50</sub>

480 Virus titrations were performed by tenfold serial dilution and end-point titration on 10<sup>4</sup>  
481 Vero/TMPRSS2/ACE2 cells per well in 96-well microtitre plates. Four days after inoculation,  
482 the CPE was analysed and the TCID<sub>50</sub> titre was calculated.

483

484 **Influenza**

485

486 Virus inactivation assay with plaque assay readout (RKI)

487 Eight µl of virus suspension (A/Panama/2007/1999 (H3N2), 1.3 × 10<sup>8</sup> PFU/ml) were added to  
488 400 µl of NCT (1.0% or 0.1% in PBS) or PBS and incubated at 37°C. After 5, 15, 30 and 60  
489 min, 100 µl were removed and added to 100 µl of met/his. As inactivation control, 100 µl of  
490 1.0% NCT were added to 100 µl of met/his and thereafter 2 µl of virus suspension were  
491 added. Infectious virus particles in all suspensions were determined with plaque assay.  
492 Briefly, a serial tenfold dilution of the virus suspension in PBS with 0.3% bovine albumin was  
493 added to confluent MDCK II cells in 12-well plates, which were washed with PBS  
494 immediately before. After incubation at 37°C for 1 h, the inoculum was removed followed by

495 a washing step with PBS. Avicel-overlay medium (double-strength MEM supplemented with  
496 0.2% BA, 1.0% DEAE dextran, 5.0% sodium bicarbonate, 1 mg/ml TPCK-trypsin and 1.25%  
497 Avicel) was added and plates incubated at 37°C and 5.0% CO<sub>2</sub> for 2 days before staining  
498 with crystal violet for visualization of plaques. Counted plaques are expressed as plaque  
499 forming units per ml (PFU/ml).

500

501 Virus inactivation assay with plaque assay readout (Hygiene and Medical Microbiology  
502 Innsbruck)

503 MDCK cells ( $2 \times 10^4$  / well) were grown in 96- well flat microtitre plates (Becton Dickinson  
504 Labware and Company, Franklin Lakes, NJ USA) for 24 h in RPMI plus 10% FCS.

505 Subsequently, the medium was replaced by 100 µl of plain RPMI per well.

506 Each viral strain (H1N1 and H1N1pdm) was tested separately. Tenfold concentrated NCT  
507 (10.0%, 5.0%, and 1.0%, respectively) in distilled water (50 µl; water without NCT for  
508 controls) was added to 450 µl of virus suspension in RPMI (pH 7.2) to a final concentration of  
509 1.0%, 0.5%, and 0.1%, respectively, and incubated for 1, 5, and 10 min at 22°C. A separate  
510 series of experiments was done with a final concentration of 0.1% NCT (5.5 mM) plus 0.1%  
511 ammonium chloride (18.7 mM) (Merck) and 1 min incubation time. At the end of the  
512 incubation time, aliquots of 100 µl were removed and mixed with 100 µl of met/his to  
513 inactivate NCT. Aliquots of 11 µl of this viral suspension in inactivated NCT were added to  
514 the MDCK cells in 96-well microtitre plates containing 100 µl RPMI per well. A series of  
515 tenfold dilutions in microtitre plates was performed. Inoculated plates were incubated at 37°C  
516 and 5.0% CO<sub>2</sub> and evaluated for plaques after 5 days. As inactivation controls, 100 µl each  
517 of 1.0% NCT and met/his were mixed. An aliquot of 50 µl was added to 450 µl of virus  
518 suspension.

519

## 520 **RSV**

521 RSV was incubated in the presence or absence of NCT at a final concentration of 0.1% and  
522 1.0% for 5, 10, 15, 30 and 60 minutes at 37°C. Virus (24 µl in DMEM plus 1.0% FCS and 2

523 mM L-glutamine) was mixed with 24  $\mu$ l of NCT in PBS. After indicated time-points, 48  $\mu$ l of  
524 met/his was added to stop the reaction. As inactivation control, NCT was preincubated with  
525 equal amount of met/his for 10 minutes at RT prior to incubation with RSV. Infectious virus  
526 particles in all samples were titrated in plaque assay using HEp2 cells as described above.  
527 Aliquots of 25  $\mu$ l were serially diluted in 100  $\mu$ l of medium (DMEM plus 10% FCS and 2 mM  
528 L-glutamine) in microtitre plates, and 100  $\mu$ l of Hep2 cells were added.

529

### 530 **Statistics**

531 Results are presented of mean values and standard deviation (SD) of generally at least three  
532 independent experiments each. Detection limits are indicated by dotted lines in the figures.  
533 Student's unpaired t-test, in cases of two groups, and one-way analysis of variance (ANOVA)  
534 and Dunnett's multiple-comparison test, in cases of more than two groups, were used to test  
535 for differences between the test and control groups. P values of  $< 0.05$  were considered  
536 significant for all tests and indicated as \*  $p < 0.05$ , \*\*  $p < 0.01$ , \*\*\*  $p < 0.001$ , \*\*\*\*  $p < 0.0001$ .  
537 Calculations were performed with GraphPad Prism 7.00 software (Graph- Pad, Inc., La Jolla,  
538 CA, USA).

539

540

541

542

543

544

545

546 **References**

- 547 1 Dhama, K. *et al.* Coronavirus Disease 2019-COVID-19. *Clinical microbiology*  
548 *reviews* **33**, doi:10.1128/cmr.00028-20 (2020).
- 549 2 Malik, Y. S. *et al.* Coronavirus Disease Pandemic (COVID-19): Challenges and a  
550 Global Perspective. *Pathogens (Basel, Switzerland)* **9**, doi:10.3390/pathogens9070519  
551 (2020).
- 552 3 Fierabracci, A., Arena, A. & Rossi, P. COVID-19: A Review on Diagnosis,  
553 Treatment, and Prophylaxis. *International journal of molecular sciences* **21**,  
554 doi:10.3390/ijms21145145 (2020).
- 555 4 World Health Organization. *Influenza (Seasonal)*, <[https://www.who.int/news-](https://www.who.int/news-room/fact-sheets/detail/influenza-(seasonal))  
556 [room/fact-sheets/detail/influenza-\(seasonal\)](https://www.who.int/news-room/fact-sheets/detail/influenza-(seasonal))> (2018).
- 557 5 Smith, D. J. *et al.* Mapping the antigenic and genetic evolution of influenza virus.  
558 *Science* **305**, 371-376, doi:10.1126/science.1097211 (2004).
- 559 6 Mitchell, J. P. *et al.* Urgent Appeal from International Society for Aerosols in  
560 Medicine (ISAM) During COVID-19: Clinical Decision Makers and Governmental  
561 Agencies Should Consider the Inhaled Route of Administration: A Statement from the  
562 ISAM Regulatory and Standardization Issues Networking Group. *Journal of aerosol*  
563 *medicine and pulmonary drug delivery* **33**, 235-238, doi:10.1089/jamp.2020.1622  
564 (2020).
- 565 7 Arentz, M. *et al.* Characteristics and Outcomes of 21 Critically Ill Patients With  
566 COVID-19 in Washington State. *Jama*, doi:10.1001/jama.2020.4326 (2020).
- 567 8 Zhou, F. *et al.* Clinical course and risk factors for mortality of adult inpatients with  
568 COVID-19 in Wuhan, China: a retrospective cohort study. *Lancet*, doi:10.1016/s0140-  
569 6736(20)30566-3 (2020).
- 570 9 Arastehfar, A. *et al.* COVID-19 Associated Pulmonary Aspergillosis (CAPA)-From  
571 Immunology to Treatment. *Journal of fungi (Basel, Switzerland)* **6**,  
572 doi:10.3390/jof6020091 (2020).
- 573 10 Koehler, P. *et al.* COVID-19 associated pulmonary aspergillosis. *Mycoses* **63**, 528-  
574 534, doi:10.1111/myc.13096 (2020).
- 575 11 Zhu, X. *et al.* Co-infection with respiratory pathogens among COVID-2019 cases.  
576 *Virus Res* **285**, 198005, doi:10.1016/j.virusres.2020.198005 (2020).
- 577 12 Aufklärung, B. f. g. *Test auf eine Infektion mit dem Coronavirus SARS-CoV-2*  
578 <[https://www.infektionsschutz.de/coronavirus/basisinformationen/test-auf-sars-cov-](https://www.infektionsschutz.de/coronavirus/basisinformationen/test-auf-sars-cov-2.html#c13339)  
579 [2.html#c13339](https://www.infektionsschutz.de/coronavirus/basisinformationen/test-auf-sars-cov-2.html#c13339)> (2020).
- 580 13 Ye, Q., Wang, B. & Mao, J. Cytokine Storm in COVID-19 and Treatment. *The*  
581 *Journal of infection*, doi:10.1016/j.jinf.2020.03.037 (2020).
- 582 14 Gottardi, W. & Nagl, M. N-chlorotaurine, a natural antiseptic with outstanding  
583 tolerability. *J. Antimicrob. Chemother* **65**, 399-409 (2010).
- 584 15 Marcinkiewicz, J. & Kontny, E. Taurine and inflammatory diseases. *Amino Acids* **46**,  
585 7-20, doi:10.1007/s00726-012-1361-4 (2014).
- 586 16 Arnitz, R. *et al.* Tolerability of inhaled N-chlorotaurine in humans – a double-blind  
587 randomized phase I clinical study. *Ther. Adv. Resp. Dis.* **12**, 1-14,  
588 doi:10.1177/1753466618778955 (2018).
- 589 17 Grisham, M. B., Jefferson, M. M., Melton, D. F. & Thomas, E. L. Chlorination of  
590 endogenous amines by isolated neutrophils. *J. Biol. Chem.* **259**, 10404-10413 (1984).
- 591 18 Weiss, S. J., Klein, R., Slivka, A. & Wei, M. Chlorination of taurine by human  
592 neutrophils. *J. Clin. Investig* **70**, 598-607 (1982).

- 593 19 Zgliczynski, J. M., Stelmaszynska, T., Domanski, J. & Ostrowski, W. Chloramines as  
594 intermediates of oxidation reaction of amino acids by myeloperoxidase. *Biochim.*  
595 *Biophys. Acta* **235**, 419-424 (1971).
- 596 20 Kim, C. & Cha, Y. N. Taurine chloramine produced from taurine under inflammation  
597 provides anti-inflammatory and cytoprotective effects. *Amino. Acids* **46**, 89-100  
598 (2014).
- 599 21 Park, E., Alberti, J., Quinn, M. R. & Schuller-Levis, G. Taurine chloramine inhibits  
600 the production of superoxide anion, IL-6 and IL-8 in activated human  
601 polymorphonuclear leukocytes. *Adv. Exp. Med. Biol* **442**, 177-182 (1998).
- 602 22 Gottardi, W. & Nagl, M. Chemical properties of N-chlorotaurine sodium, a key  
603 compound in the human defence system. *Arch. Pharm. Pharm. Med. Chem.* **335**, 411-  
604 421 (2002).
- 605 23 Gottardi, W., Debabov, D. & Nagl, M. N-chloramines: a promising class of well-  
606 tolerated topical antiinfectives. *Antimicrob. Agents Chemother.* **57**, 1107-1114 (2013).
- 607 24 Nagl, M., Arnitz, R. & Lackner, M. N-Chlorotaurine, a Promising Future Candidate  
608 for Topical Therapy of Fungal Infections. *Mycopathologia* **183**, 161-170,  
609 doi:10.1007/s11046-017-0175-z (2018).
- 610 25 Garcia, L. A. T., Boff, L., Barardi, C. R. M. & Nagl, M. Inactivation of adenovirus in  
611 water by natural and synthetic compounds *Food and Environmental Virology* **11**, 157-  
612 166, doi:10.1007/s12560-019-09370-8 (2019).
- 613 26 Huemer, H. P., Nagl, M. & Irschick, E. U. In vitro prevention of vaccinia and herpes  
614 virus infection spread in explanted human corneas by N-chlorotaurine. *Ophthalmic.*  
615 *Res.* **43**, 145-152 (2010).
- 616 27 Nagl, M., Larcher, C. & Gottardi, W. Activity of N-chlorotaurine against herpes  
617 simplex- and adenoviruses. *Antiviral Res* **38**, 25-30 (1998).
- 618 28 Dudani, A. K., Martyres, A. & Fliss, H. Short communication: rapid preparation of  
619 preventive and therapeutic whole-killed retroviral vaccines using the microbicide  
620 taurine chloramine. *AIDS Res. Hum. Retroviruses* **24**, 635-642 (2008).
- 621 29 Kyriakopoulos, A. M., Logotheti, S., Marcinkiewicz, J. & Nagl, M. N-chlorotaurine  
622 and N-bromotaurine combination regimen for the cure of valacyclovir-unresponsive  
623 herpes zoster comorbidity in a multiple sclerosis patient. *International Journal of*  
624 *Medical and Pharmaceutical Case Reports* **7**, 1-6, doi:10.9734/IJMPCR/2016/25476  
625 (2016).
- 626 30 Romanowski, E. G. *et al.* N-chlorotaurine is an effective antiviral agent against  
627 adenovirus in vitro and in the Ad5/NZW rabbit ocular model. *Invest. Ophthalmol. Vis.*  
628 *Sci.* **47**, 2021-2026 (2006).
- 629 31 Teuchner, B. *et al.* Tolerability and efficacy of N-chlorotaurine in epidemic  
630 keratoconjunctivitis – a double-blind randomized phase 2 clinical trial. *J. Ocul.*  
631 *Pharmacol. Ther.* **21**, 157-165 (2005).
- 632 32 Jekle, A. *et al.* Broad-spectrum virucidal activity of (NVC-422) N,N-dichloro-2,2-  
633 dimethyltaurine against viral ocular pathogens in vitro. *Invest. Ophthalmol. Vis. Sci.*  
634 **54**, 1244-1251 (2013).
- 635 33 Leiter, H. *et al.* Microbicidal activity of N-chlorotaurine can be enhanced in the  
636 presence of lung epithelial cells *Journal of Cystic Fibrosis*,  
637 doi:10.1016/j.jcf.2020.03.005 (2020).
- 638 34 Geiger, R. *et al.* Tolerability of inhaled N-chlorotaurine in the pig model. *BMC*  
639 *Pulmon. Med.* **9**, 33 (2009).
- 640 35 Nagl, M. *et al.* Tolerability of inhaled N-chlorotaurine versus sodium chloride in the  
641 mouse. *J. Med. Res. Pract.* **2**, 163-170 (2013).
- 642 36 Schwienbacher, M. *et al.* Tolerability of inhaled N-chlorotaurine in an acute pig  
643 streptococcal lower airway inflammation model. *BMC Infect. Dis.* **11**, 231 (2011).

- 644 37 Yoon, J. *et al.* Virucidal mechanism of action of NVC-422, a novel antimicrobial drug  
645 for the treatment of adenoviral conjunctivitis. *Antiviral Res* **92**, 470-478 (2011).
- 646 38 Gottardi, W. & Nagl, M. Chlorine covers on living bacteria: the initial step in  
647 antimicrobial action of active chlorine compounds. *J. Antimicrob. Chemother* **55**, 475-  
648 482 (2005).
- 649 39 Eitzinger, C. *et al.* N-chlorotaurine, a long-lived oxidant produced by human  
650 leukocytes, inactivates Shiga toxin of enterohemorrhagic *Escherichia coli*. *PloS One*  
651 **7**, e47105 (2012).
- 652 40 Jekle, A. *et al.* NVC-422 inactivates *Staphylococcus aureus* toxins. *Antimicrob.*  
653 *Agents Chemother* **57**, 924-929 (2013).
- 654 41 Nagl, M. *et al.* Impact of N-chlorotaurine on viability and production of secreted  
655 aspartyl proteinases of *Candida* spp. *Antimicrob. Agents Chemother.* **46**, 1996-1999  
656 (2002).
- 657 42 Reeves, E. P., Nagl, M., O'Keeffe, J., Kelly, J. & Kavanagh, K. Effect of N-  
658 chlorotaurine on *Aspergillus*, with particular reference to destruction of secreted  
659 gliotoxin. *J. Med. Microbiol* **55**, 913-918 (2006).
- 660 43 Sauerbrei, A. *et al.* Sensitivity of human adenoviruses to different groups of chemical  
661 biocides. *J Hosp. Infect* **57**, 59-66 (2004).
- 662 44 Kramer, A. *et al.* Consensus on Wound Antisepsis: Update 2018. *Skin pharmacology*  
663 *and physiology* **31**, 28-58, doi:10.1159/000481545 (2018).
- 664 45 McDonnell, G. & Russell, A. D. Antiseptics and disinfectants: activity, action, and  
665 resistance. *Clin. Microbiol. Rev* **12**, 147-179 (1999).
- 666 46 Gottardi, W., Arnitz, R. & Nagl, M. N-chlorotaurine and ammonium chloride: an  
667 antiseptic preparation with strong bactericidal activity. *Int. J. Pharm.* **335**, 32-40  
668 (2007).
- 669 47 Gruber, M., Moser, I., Nagl, M. & Lackner, M. Bactericidal and fungicidal activity of  
670 N-chlorotaurine is enhanced in cystic fibrosis sputum medium. *Antimicrob. Agents*  
671 *Chemother.* **61**, 1-10, doi:10.1128/AAC.02527-16 (2017).
- 672 48 Böttcher, B., Sarg, B., Lindner, H. H. & Nagl, M. Inactivation of microbicidal active  
673 halogen compounds by sodium thiosulphate and histidine/methionine for time-kill  
674 assays. *J. Microbiol. Methods* **141**, 42-47, doi:10.1016/j.mimet.2017.07.014 (2017).
- 675 49 Hoffmann, M. *et al.* SARS-CoV-2 Cell Entry Depends on ACE2 and TMPRSS2 and  
676 Is Blocked by a Clinically Proven Protease Inhibitor. *Cell* **181**, 271-280.e278,  
677 doi:10.1016/j.cell.2020.02.052 (2020).
- 678 50 Ternette, N., Tippler, B., Uberla, K. & Grunwald, T. Immunogenicity and efficacy of  
679 codon optimized DNA vaccines encoding the F-protein of respiratory syncytial virus.  
680 *Vaccine* **25**, 7271-7279, doi:10.1016/j.vaccine.2007.07.025 (2007).
- 681 51 Reed, L. J. & Muench, H. A simple method of estimating fifty percent endpoints.  
682 *American Journal of Epidemiology* **27**, 493-497,  
683 doi:10.1093/oxfordjournals.aje.a118408 (1938).
- 684 52 Shatzkes, K., Teferedegne, B. & Murata, H. A simple, inexpensive method for  
685 preparing cell lysates suitable for downstream reverse transcription quantitative PCR.  
686 *Scientific reports* **4**, 4659, doi:10.1038/srep04659 (2014).
- 687 53 Corman, V. M. *et al.* Detection of 2019 novel coronavirus (2019-nCoV) by real-time  
688 RT-PCR. *Euro surveillance : bulletin Europeen sur les maladies transmissibles =*  
689 *European communicable disease bulletin* **25**, doi:10.2807/1560-  
690 7917.Es.2020.25.3.2000045 (2020).

691

692



693

**694 Acknowledgements**

695 We are grateful to Andrea Windisch for excellent technical assistance in the production of  
696 NCT and to Thomas Grunwald and Leila Issmail, Fraunhofer Institute for Cell Therapy and  
697 Immunology, Leipzig, Germany, for provision of and technical support with the RSV. We  
698 thank Brian Monk (Otago University, Dunedin, New Zealand) and Ian Monk (Doherty  
699 Institute, Melbourne, Australia) for establishing the connection with 360biolabs, Melbourne,  
700 Australia.

701

**702 Author Contributions**

703 A.R., A.V., M.S., T.W., A.L., J.F. and H.S. performed the assays against SARS-CoV-2, M.S.,  
704 T.W., J.S. and M.N. the assays against influenza viruses, B.M. and Z.B. the assays against  
705 RSV. M.L., M.N., C.S., D.v.L., planned the work, made the concept and guided the work.  
706 M.N. and M.L. wrote the manuscript under contribution of all other authors. All authors edited  
707 and approved the manuscript.

708

**709 Funding**

710 This study was supported by the German Federal Ministry of Education and Research  
711 (BMBF) grants 'NUM Organo-Strat' and 'BUA Coronavirus Exploration project'.

712

713

**714 Competing Interests statement**

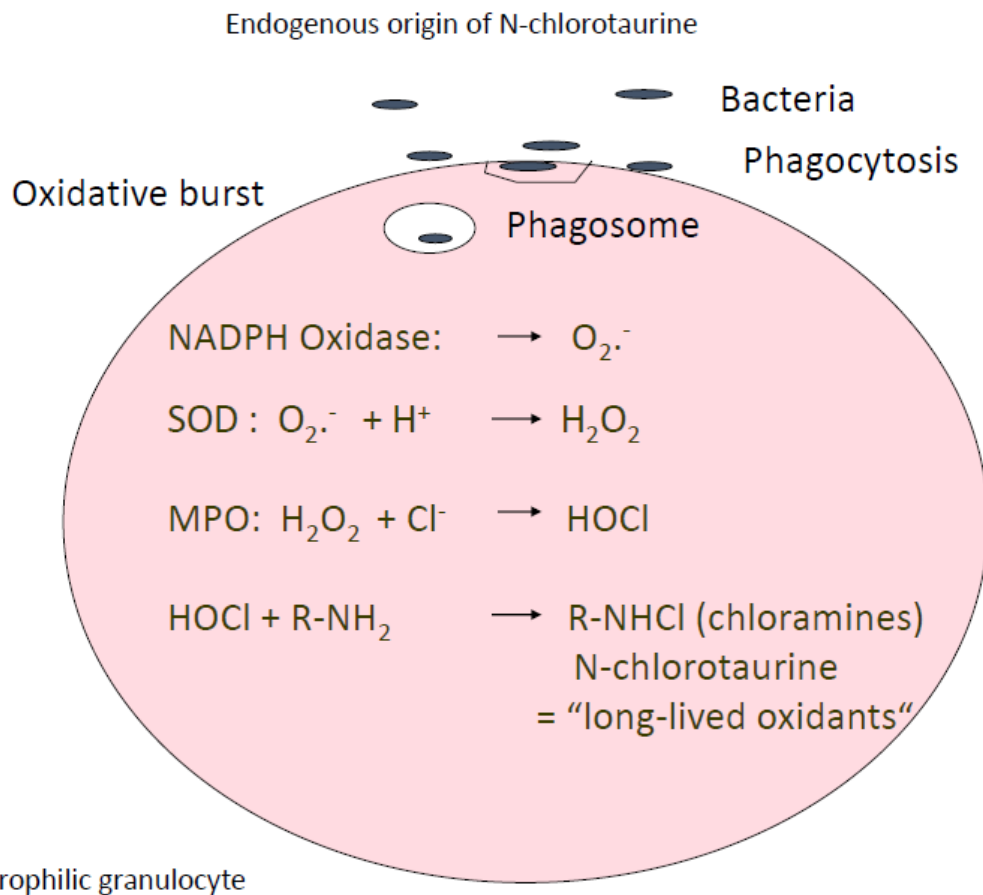
715 M. Nagl is co-inventor of a patent on the application of NCT for inhalation (EP 2265267 B1).  
716 All other authors declare no conflict of interest.

717



719 **Figures**

720



721

722

723 Fig. 1

724

725 **Fig. 1: Endogenous origin of NCT.**

726 NCT is formed in activated human granulocytes and monocytes via an enzymatic cascade,

727 the oxidative burst. Subsequent to superoxide ( $O_2^{\cdot-}$ ) and hydrogen peroxide ( $H_2O_2$ ), the

728 highly reactive hypochlorite (HOCl) is created by myeloperoxidase (MPO), which among

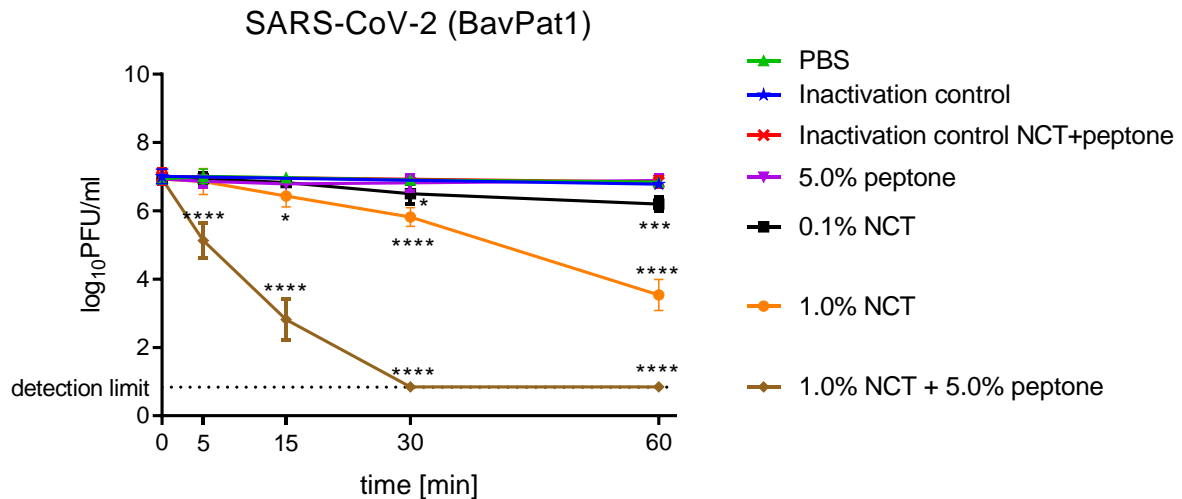
729 others reacts with amino compounds to form less reactive chloramines, also named long-

730 lived oxidants. NCT is the main representative of these chloramines. SOD superoxide

731 dismutase.

732

733



734

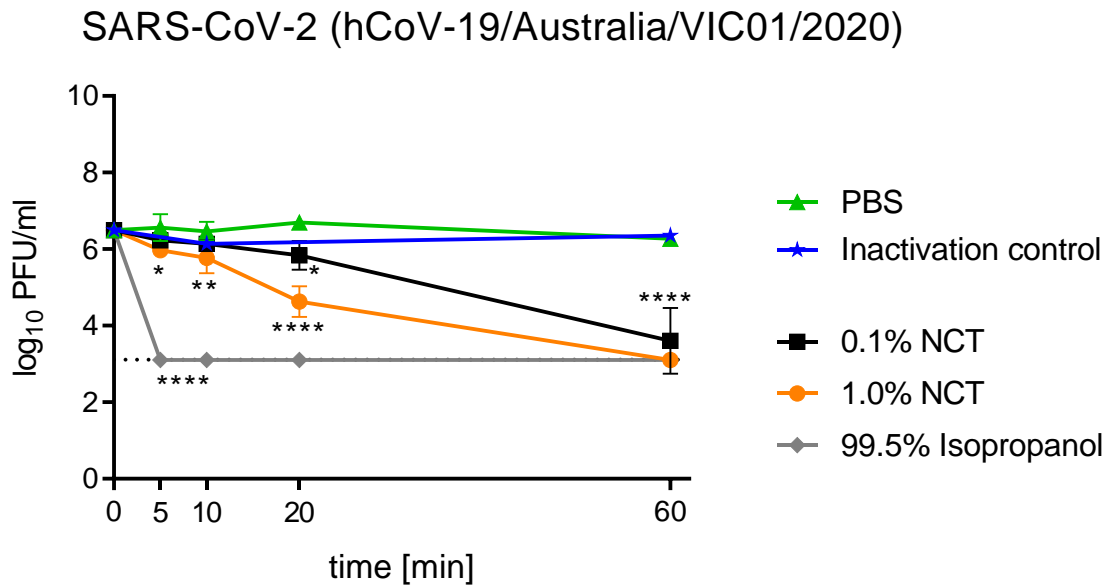
735 Fig. 2a

736

737 **Fig. 2: Inactivation of SARS-CoV-2 by NCT.**

738 a, Virus suspension (SARS-CoV-2 BavPat1) was incubated with 1.0% (55 mM) NCT, 0,1%  
 739 (5.5 mM) NCT, 1.0% NCT with 5.0% peptone or PBS or 5.0% peptone for 5 min, 15 min, 30  
 740 min, or 60 min at 37°C, after which samples were diluted 1:1 in met/his solution for  
 741 inactivation of NCT. Remaining infectious virus particles were determined using plaque  
 742 titration. To control for inactivation of NCT by met/his, virus was added after dilution of 1.0%  
 743 NCT with or without peptone in met/his. Mean values  $\pm$  SD of three to eight independent  
 744 experiments in duplicates. The dotted line indicates the detection limit (0.84 log<sub>10</sub>). Data were  
 745 statistically analysed using a two-way ANOVA including a Dunnett's multiple comparison test  
 746 to PBS controls. \*  $p < 0.05$ , \*\*  $p < 0.01$ , \*\*\*  $p < 0.001$ , \*\*\*\*  $p < 0.0001$ . Of note, the  
 747 inactivation of the virus by NCT was markedly enhanced in the presence of peptone.

748



749

750 Fig. 2b

751

752 **Fig. 2: Inactivation of SARS-CoV-2 by NCT.**

753 **b**, Virus suspension (SARS-CoV-2 h CoV-19/Australia/VIC01/2020) was incubated with NCT  
 754 or PBS or isopropanol (positive control) for 5 min, 10 min, 20 min, and 60 min at 37°C and  
 755 then diluted 1:1 in met/his for inactivation of NCT, followed by plaque titration. Mean values ±  
 756 SD of three independent experiments. Detection limit 3.11 log<sub>10</sub> (dotted line).

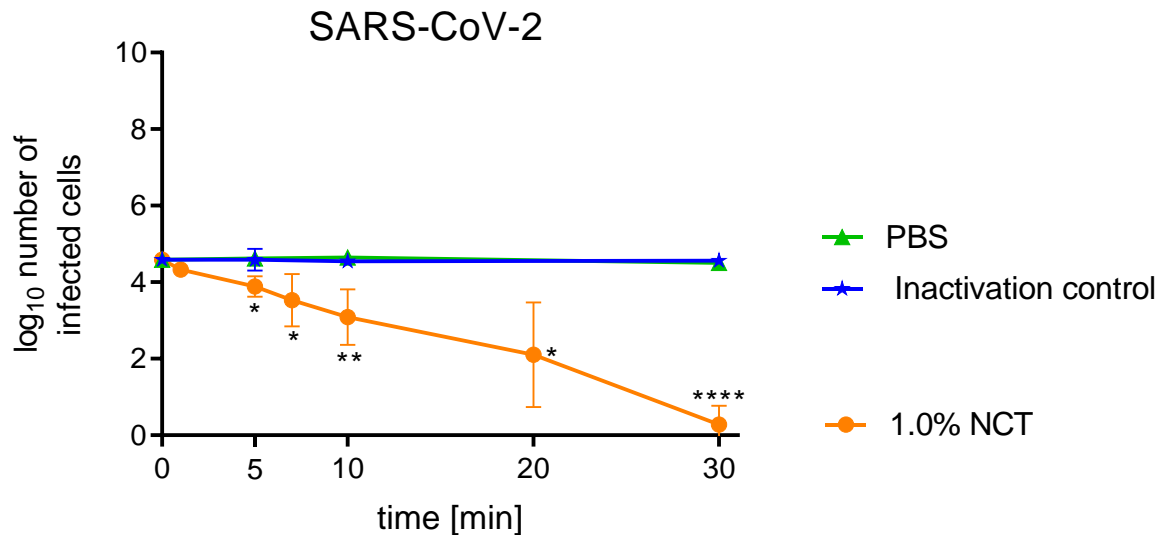
757

758

759

760

761



762

763

764 Fig. 2c

765

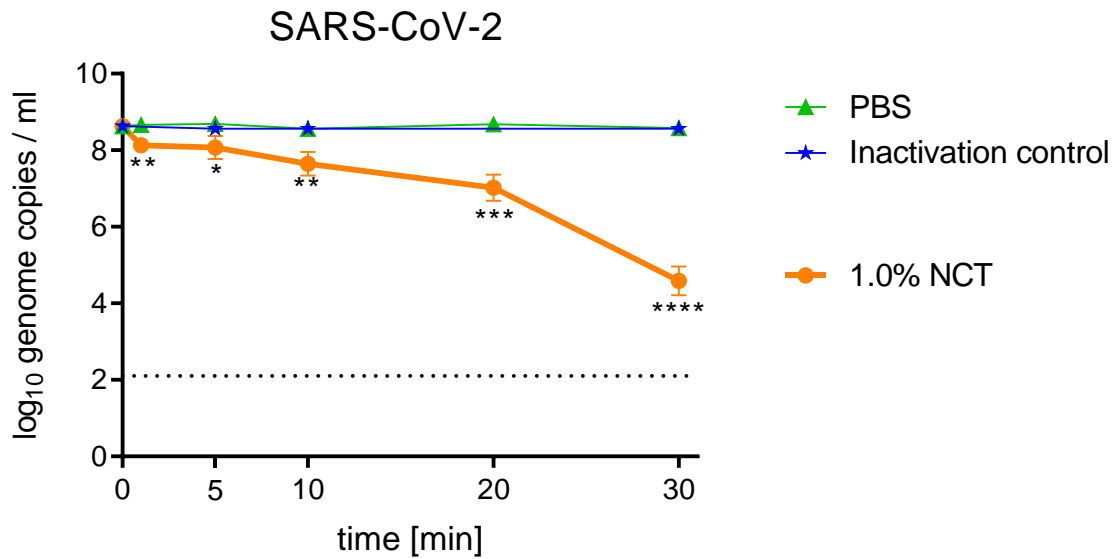
766 **Fig. 2: Inactivation of SARS-CoV-2 by NCT.**

767 **c**, Virus suspension (SARS-CoV-2, clinical isolate) was incubated with 1% NCT or PBS for 1  
768 min, 5 min, 7 min, 10 min, 20 min, and 30 min at 37°C. After inactivation of NCT and serial  
769 dilution, aliquots were added to Vero/TMPRSS2/ACE2 cells for 1 h in 96-well plates. Cells  
770 were washed, incubated for further 9 h, and fixed for Immunostaining (**c**) or RT-qPCR (**d**). In  
771 immunostaining, infected cells were visible as red spots and counted using an ImmunoSpot  
772 S6 Ultra-V reader and CTL analyser *BioSpot*® 5.0 software. Mean values  $\pm$  SD of three  
773 independent experiments.

774

775

776



777

778

779 Fig. 2d

780

781 **Fig. 2: Inactivation of SARS-CoV-2 by NCT.**782 **d**, After cell lysis and RNA extraction, one-step RT-qPCR assay was performed using the

783 iTaq™ RT-PCR (BIO-RAD) kit and previously published primers and probes specific for

784 detection of the SARS-CoV-2 E Gene on a CFX96™ real-time system (BIO-RAD). Mean

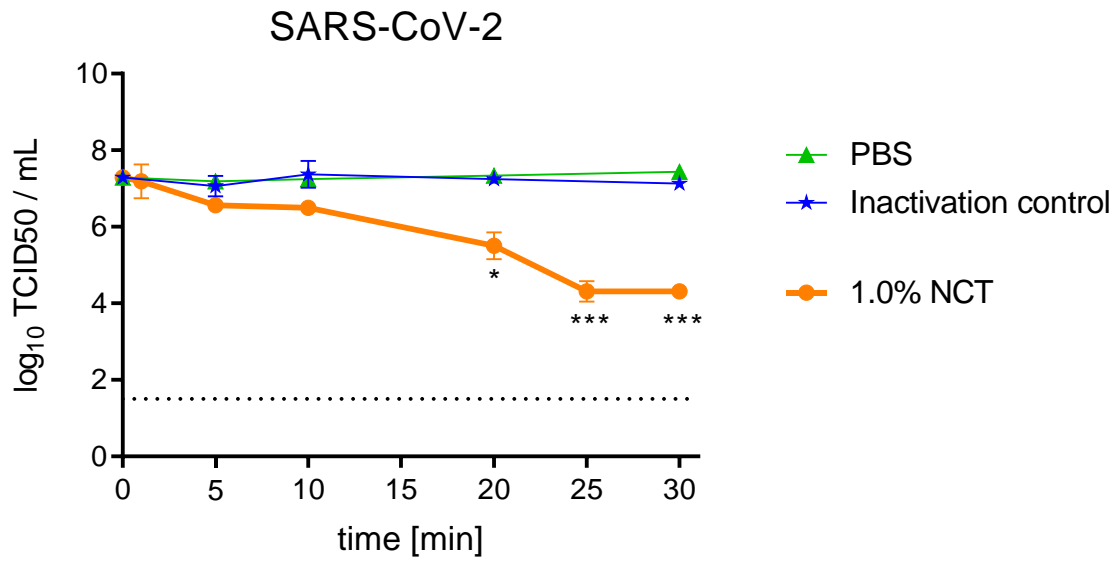
785 values ± SD of genome copies of three independent experiments. Detection limit 2.10 log<sub>10</sub>

786 RNA copies/ml (dotted line).

787

788

789



790

791 Fig. 2e

792

793 **Fig. 2: Inactivation of SARS-CoV-2 by NCT.**794 e, Virus titration by TCID<sub>50</sub>. Mean values ± SD of two independent experiments. Detection795 limit 1.50 log<sub>10</sub> (dotted line).

796

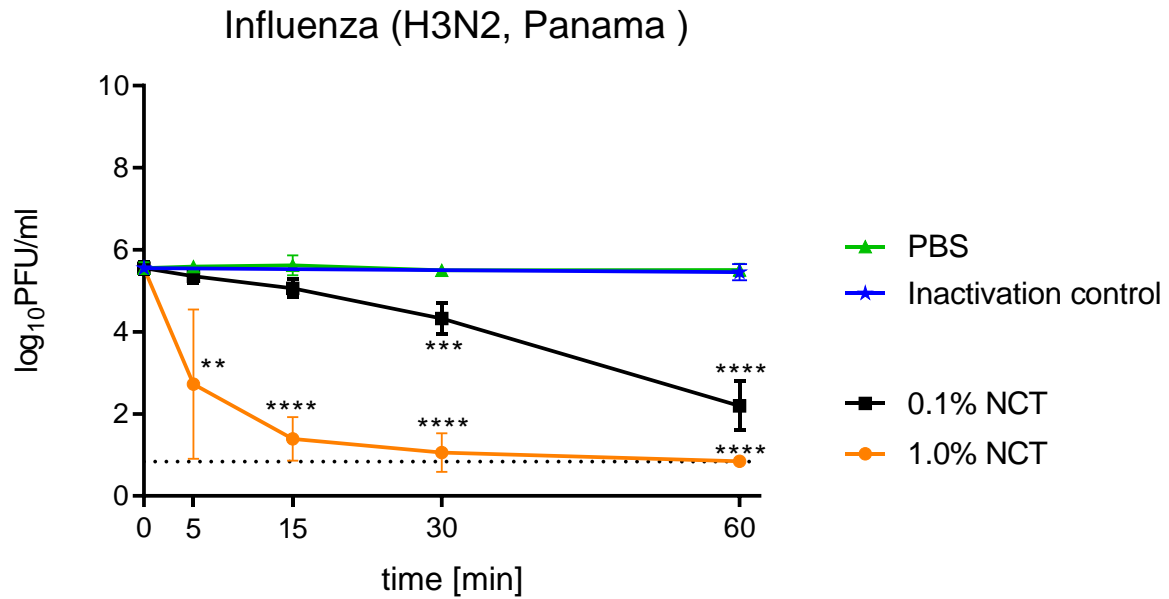
797

798

799



800



801

802

803 Fig. 3a

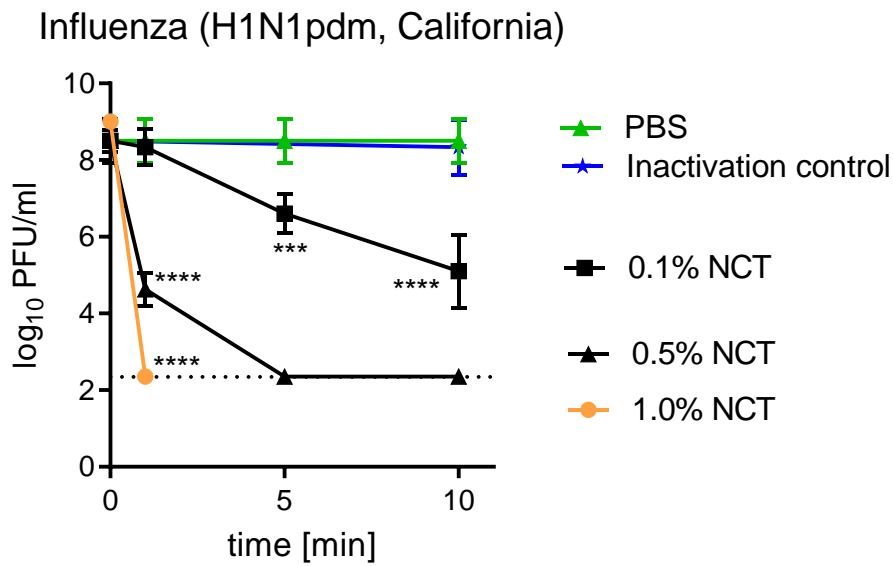
804

805 **Fig. 3: Inactivation of influenza viruses by NCT.**

806 a, Inactivation of Influenza A/Panama/2007/1999 (H3N2) by 1.0% (55 mM) and 0.1% (5.5  
 807 mM) NCT. Virus suspension was incubated with NCT or PBS for 5 min, 15 min, 30 min, or 60  
 808 min at 37°C, after which samples were diluted 1:1 in met/his solution for inactivation of NCT.  
 809 Remaining infectious virus particles were determined using plaque titration. To control for  
 810 inactivation of NCT by met/his, virus was added after dilution of 1.0% NCT in met/his in the  
 811 inactivation control. Mean values  $\pm$  SD of five independent experiments. \*  $p < 0.05$ , \*\*  $p <$   
 812  $0.01$ , \*\*\*  $p < 0.001$ , \*\*\*\*  $p < 0.0001$  versus PBS control. Detection limit  $0.84 \log_{10}$  (dotted  
 813 line).

814

815



816

817

818 Fig. 3b

819

820 **Fig. 3: Inactivation of influenza viruses by NCT.**

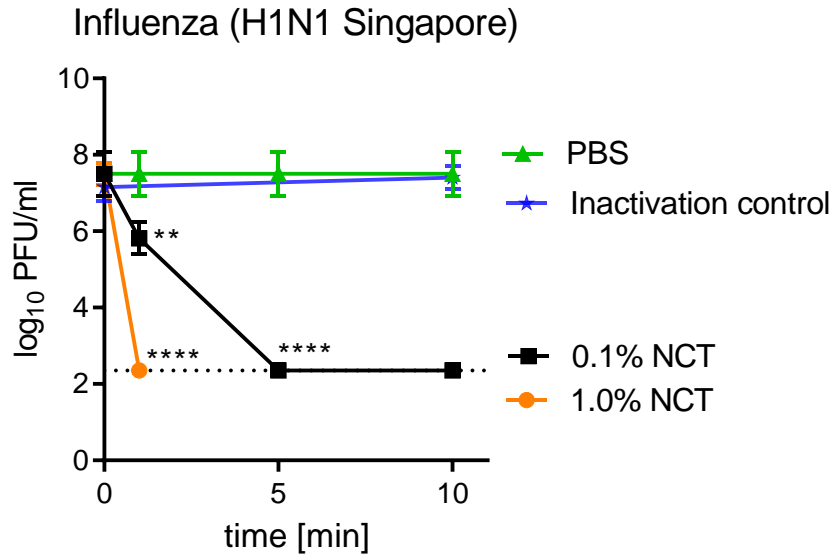
821 **b**, Inactivation of Influenza A/California/ Swine Origin Virus/2009 (H1N1pdm) by 0.1%, 0.5%  
 822 and 1.0% NCT.

823 Virus suspension was incubated with NCT in RPMI or plain RPMI for 1 min, 5 min, and 10  
 824 min at 22°C, after which samples were diluted 1:1 in met/his solution for inactivation of NCT.

825 Remaining infectious virus particles were determined using plaque titration. Mean values  $\pm$   
 826 SD of four independent experiments. Detection limit 2.35 log<sub>10</sub> (dotted line).

827

828



829

830

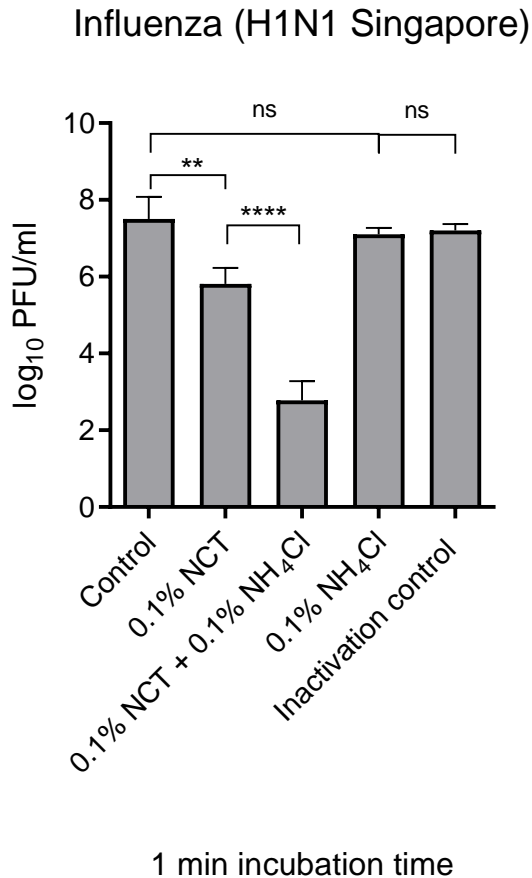
831 Fig. 3c

832

833 **Fig. 3: Inactivation of influenza viruses by NCT.**834 **c**, Inactivation of Influenza A/Singapore/Hongkong/2339/2000 (H1N1) by 0.1% and 1.0%835 NCT and **(d)** by 0.1% NCT and 0.1% (5.5 mM) NCT plus 0.1% (18.7 mM) ammonium

836 chloride compared. Test procedure and number of independent experiments as in Fig. 3b.

837



838

839 Fig. 3d

840

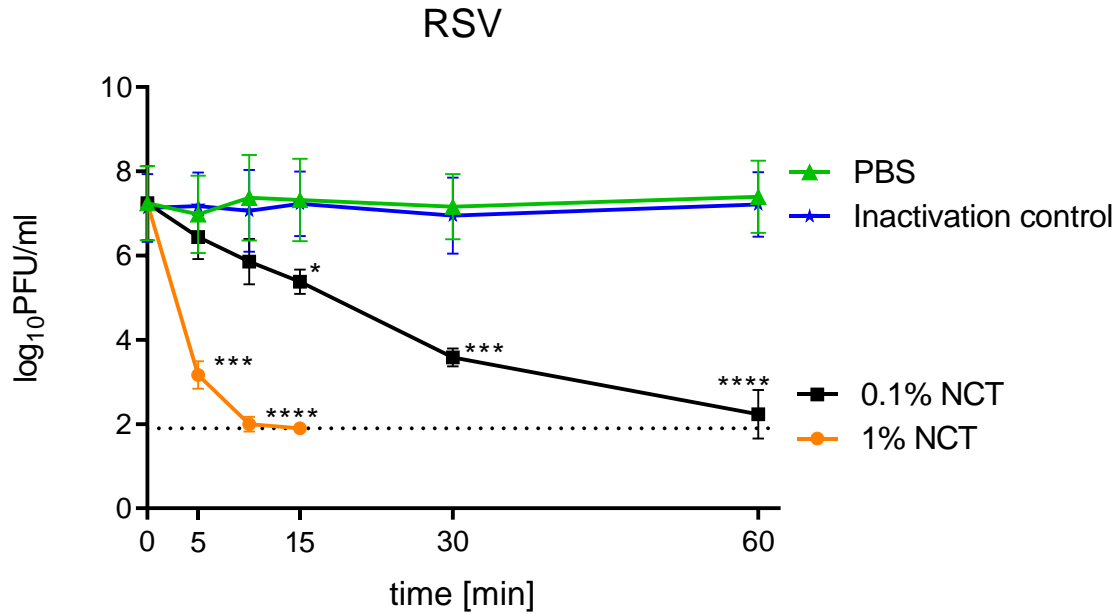
841 **Fig. 3: Inactivation of influenza viruses by NCT.**842 **c**, Inactivation of Influenza A/Singapore/Hongkong/2339/2000 (H1N1) by 0.1% and 1.0%843 NCT and **(d)** by 0.1% NCT and 0.1% (5.5 mM) NCT plus 0.1% (18.7 mM) ammonium

844 chloride compared. Test procedure and number of independent experiments as in Fig. 3b.

845 Inactivation control in **(d)** consisting of 0.1% NCT plus 0.1% NH<sub>4</sub>Cl plus inactivator.

846

847



848

849

850 Fig. 4

851

852 **Fig. 4: Inactivation of respiratory syncytial virus by NCT.**

853 Virus suspension was incubated with 1.0% or 0.1% NCT or PBS for 5 min, 10 min, 15 min,

854 30 min, or 60 min at 37°C, after which samples were diluted 1:1 in met/his solution for

855 inactivation of NCT. Remaining infectious virus particles were determined using plaque

856 titration. Mean values  $\pm$  SD of three independent experiments. Detection limit 1.90 log<sub>10</sub>

857 (dotted line).

858

859